Journal of the Serbian Chemical Society
JSCS-info@shd.org.rs • www.shd.org.rs/JSCS
J. Serb. Chem. Soc. 77 (11) 1609–1623 (2012)
JSCS–4375
UDC 546.57+549.753.11–36:621.793:620.193:66.022.362
Original scientific paper

Electrochemical impedance spectroscopy of a silver-doped hydroxyapatite coating in simulated body fluid used as a corrosive agent

ANA JANKOVIĆ[1#], SANJA ERAKOVIĆ[1#], ANTONIJA DINDUNE[2], DJORDJE VELJOVIĆ[1#], TATJANA STEVANOVIĆ[3], DJORDJE JANAĆKOVIĆ[1#] and VESNA MIŠKOVIĆ-STANKOVIĆ[1#*]

[1]Faculty of Technology and Metallurgy, University of Belgrade, Karnegijeva 4, 11000 Belgrade, Serbia, [2]Institute of Inorganic Chemistry, Riga Technical University, 34 Miera Street, Salaspils, LV-2169, Latvia and [3]Département des sciences du bois et de la forêt, Université Laval, 2425 rue de la Terrasse, Québec, Canada

(Received 12 July, revised 27 August 2012)

Abstract: Titanium is a key biomedical material due to its good biocompatibility, mechanical properties and corrosion stability, but infections at the implantation site still pose a serious threat. One approach to prevent infection is to improve the antimicrobial ability of the coating material. Silver-doped hydroxyapatite (Ag/HAP) nanoparticles were synthesized by a new modified precipitation method. The synthesized powder was used for the preparation of Ag/HAP coating on titanium by electrophoretic deposition. The coating was characterized in terms of phase composition and structure by attenuated total reflection Fourier transform infrared spectroscopy (ATR–FTIR) and X-ray diffraction (XRD); the surface morphology and chemical composition was assessed using scanning electron microscopy (SEM) and energy dispersive spectroscopy (EDS). The research focused on an evaluation of the corrosion behaviour of Ag/HAP coating in simulated body fluid (SBF) at 37 °C during prolonged immersion time by electrochemical impedance spectroscopy (EIS). The silver-doped HAP coating provided good corrosion protection in SBF solution.

Keywords: electrochemical impedance; hydroxyapatite; silver; electrophoretic deposition; simulated body fluid.

INTRODUCTION

Titanium still holds a pivotal role for most biomedical applications, primarily as orthopaedic and dental implant material, thanks to its excellent biocompatibility and mechanical properties.[1] The key feature that enables such a wide-

* Corresponding author. E-mail: vesna@tmf.bg.ac.rs
# Serbian Chemical Society member.
doi: 10.2298/JSC120712086J

spread implementation is its excellent corrosion stability. A stable oxide layer that forms spontaneously upon exposure to oxygen is believed to be 3–10 nm thick, thus providing low electronic conductivity and high corrosion resistance.[2,3] The same oxide layer provides a good substrate for adhesion of proteins and cells, precursors for osteogenesis in the vicinity of an implant. Nevertheless, the same property is to blame for biofilm formation on the implant/tissue interface, which usually consists of various microorganisms, such as pathogenic bacteria. Bacterial infection of the implantation site inevitably leads to post-op complications, revision surgeries, implant failure and finally complete removal.

Antibacterial coatings on titanium can be divided into several groups based on their most prominent feature: coatings loaded with antibiotics, coatings containing non-antibiotic antimicrobial agents, coatings containing inorganic antimicrobial agents, adhesion resistant coatings, *etc*.[4] Recently, due to their excellent biocompatibility and stability, attention has been drawn to inorganic antimicrobial agents, silver in particular. The advantages of silver and the silver ion as doping agents are that they inhibit initial bacterial attachment onto biomaterials; the effect is long lasting, and they have a broad antibacterial spectrum at low concentrations. Studies have shown that Ag has excellent biocompatibility without genotoxicity or cytotoxicity, although its mechanism of action is still not completely revealed. Due to its stability, it can be introduced by various techniques (physical vapour deposition, magnetron sputtering, electrophoretic deposition, to name a few). Lastly, silver can be used for doping a variety of biomaterials (ceramics, metals, polymers) and especially Ag has generated great interest in the development of silver-doped hydroxyapatite coatings.

Hydroxyapatite (HAP) [$Ca_{10}(PO_4)_6(OH)_2$] represents a crystallo-chemical analogue of the mineral bone component and has been long used as part of the synthetic materials for orthopaedic implants.[5–9] The titanium implant fixation properties are dramatically enhanced when coated with HAP.[7–9] The release of metal ions into the body can be reduced by suitable biocompatible inorganic coatings, such as hydroxyapatite (HAP), and this can lead to a delay in corrosion, and wear, and also minimize the loosening of implants from the bone. HAP is not only bioactive, but also osteoconductive, non-toxic and non-immunogenic. However, the most striking property of inorganic HAP is its ability to form an apatite layer, similar to bone apatite, on the surface of implants. The coating surface that aids the process of HAP precipitation by firmly anchoring hydroxyapatite on the surface, thus accelerating and securing a direct bond of the implant with bone is known as bioactive.

Among different methods of ceramic coating deposition on a metal surface, such as plasma spraying, sputtering, pulsed laser-deposition, sol–gel, electrophoresis and electrodeposition, electrophoretic deposition (EPD) has emerged as the most suitable one.[10] EPD provides for uniform coatings, even on substrates

of complex shape. Other advantages are that this is an inexpensive electrochemical technique that can be performed at room temperature with a relatively simple set-up. Coating thickness and morphology are well controlled by adjusting the deposition parameters.[11,12]

This paper reports on an investigation of the *in vitro* biological compatibility and corrosion stability of a non-sintered Ag/HAP coating on titanium obtained by electrophoretic deposition, after immersion in SBF solution at 37 °C, with the aim of mimicking human body conditions.

EXPERIMENTAL

Synthesis of hydroxyapatite powder doped with silver

A modified chemical precipitation method was employed for the preparation of a silver/hydroxyapatite powder. Calcium oxide, obtained by aerobic calcination of $CaCO_3$ for 5 h at 1000 °C, was subsequently placed in a reaction vessel with silver nitrate and phosphoric acid. The reaction was conducted in a stepwise manner. The stoichiometric amount of the resulting calcium oxide was mixed and stirred in distilled water for 10 min. In the second step $AgNO_3$ solution, up to 0.4±0.1 wt. % final concentration, was added to the suspension. Lastly, phosphoric acid was added drop-wise to the suspension in order to obtain silver-doped hydroxyapatite, $Ca_{9.95}Ag_{0.05}(PO_4)_6(OH)_2$. Upon addition of the total stoichiometric volume of phosphoric acid, the pH reached a value of 7.4–7.6. The final suspension was heated for 30 min at 94±1 °C and stirred for another 30 min. After sedimentation, the upper clear solution layer was separated from the precipitate by decanting. In the final step, the suspension was spray-dried at 120±5 °C into a granulated powder.

Surface preparation of titanium

Two different dimensions of titanium plates were used, (25 mm×10 mm×0.89 mm) for surface analysis and (40 mm×20 mm×0.25 mm) for impedance measurements, both from Aldrich (purity 99.7 %). The pure Ti foils represented substrates for the cathodic deposition of the Ag/HAP coatings. Before deposition, standard mechanical pre-treatment of metal plates was employed. Grit emery paper was used to polish the Ti plates, followed by wet polishing with 0.3 μm alumina. After polishing, the plates were degreased, first in acetone and then in ethanol for 15 min, both in an ultrasonic bath.

Electrophoretic deposition of Ag/HAP coating

Electrophoretic deposition was performed from 100 ml of absolute ethanol suspension containing 1.0034 g of nano-sized Ag/HAP powder. Homogeneous and stable suspension was obtained by ultrasonic pre-treatment for 15 min. To increase the suspension stability, hydrochloric acid (HCl) was added dropwise until a pH value of 2.00 was attained. Low pH values of the suspension are necessary to keep the colloidal particles positively charged.[13] The effective pH value of 2 was chosen based on optimization of the experimental conditions to obtain the most stable suspension. Prior to electrodeposition, the ethanol Ag/HAP suspension was ultrasonicated for 30 min to obtain a homogeneous suspension.

A three-electrode cell arrangement was used for the cathodic electrodeposition. The working electrode (pre-treated titanium plate) was used as a substrate for the deposition of an Ag/HAP coating. The counter electrodes were two pure platinum panels, placed parallel to the Ti plate at a distance of 1.5 cm.

The coatings were acquired on the titanium from ethanolic Ag/HAP suspension, using the constant voltage method. The experiments were performed at a constant voltage of 60 V for a deposition time of 45 s, at room temperature. Electrodeposited Ag/HAP coatings were air dried for 24 h at room temperature.

Methods for structural and electrochemical analysis

X-Ray diffraction. A Philips PW 1051 powder diffractometer with Ni-filtered Cu K_α radiation (λ = 1.5418 Å) was employed for X-ray diffraction (XRD) assessment of the phase composition of the electrodeposited coatings. The diffraction intensity was measured using the scan-step technique in the 2θ range of 8–80° with a scanning step width of 0.05° and exposition time of 50 s per step. The phase analysis was realised using the PDF-2 database with a commercially available computer program, EVA V.9.0.

Scanning electron microscopy with energy dispersive spectroscopy. A JEOL JSM-5800 scanning electron microscope (SEM), operated at 20 keV, equipped for energy dispersive spectroscopy (EDS) measurements, was used to analyze the morphology of the electrodeposited coatings.

Attenuated total reflection Fourier transform infrared spectroscopy. A Spectrum^{TM} 400 Perkin Elmer infrared spectrometer (USA) instrument was used to perform the attenuated total reflection Fourier transforms infrared spectroscopy (ATR–FTIR) measurements. Scanning was performed in the 600–4000 cm^{-1} wavelength range in order to investigate the functional groups present in the electrodeposited coatings.

Thermogravimetric analysis. The thermal behaviour of the electrodeposited coatings, dried at room temperature and then scraped from the titanium substrate, was examined by the thermogravimetric analysis (TGA) on a Mettler Toledo instrument (TGA/SDTA851e). Scans were recorded in the dynamic mode from 25 to 1000 °C at a heating rate of 20 °C min^{-1}, under a nitrogen atmosphere (flow rate 50 ml min^{-1}). For each experiment, about 5 mg of oven-dried sample were used.

Electrochemical impedance spectroscopy. For the electrochemical impedance spectroscopy (EIS) measurements, an electrodeposited Ag/HAP coating and bare titanium, as a control, were exposed to SBF solution at 37 °C for 72 h. A standard three-electrode cell arrangement was used in the experiments. The SBF solution (Table I) was prepared by dissolving reagent-grade salts in deionised water followed by buffering with tris-hydroxymethyl aminomethane. The final pH value was adjusted to 7.40 (at 37 °C) using 1 M hydrochloric acid. The working electrode was coated titanium or thermally untreated bare titanium (tested surface area of 1 cm^2). The counter electrode was a platinum mesh and the reference electrode was a saturated calomel electrode (SCE). The impedance data were obtained at the open-circuit po-

TABLE I. Composition of the SBF solution similar to human blood plasma

Reagent	c / g dm^{-3}
NaCl	7.996
$NaHCO_3$	0.350
KCl	0.224
$K_2HPO_4 \cdot 3H_2O$	0.228
$MgCl_2 \cdot 2H_2O$	0.305
$CaCl_2$	0.278
Na_2SO_4	0.071
$(CH_2OH)_3CNH_2$	6.057
1 M HCl	40 ml

tential using a Reference 600^{TM} potentiostat/galvanostat/ZRA (Gamry Instruments, Inc., Warminister, PA, USA), over a frequency range of 300 kHz to 10 mHz using 5 mV amplitude of the sinusoidal voltage. The impedance spectra were analyzed using Gamry Instruments Echem Analyst fitting program, version 5.50.

RESULTS AND DISCUSSION

XRD Analysis

XRD analysis of electrodeposited Ag/HAP coating on titanium was performed in order to determine the phase composition and structural changes of silver/hydroxyapatite. HAP high intensity peaks are dominant in the spectrum (Fig. 1) and perfectly match the hydroxyapatite pattern (JCPDS 86–1199). The incorporation of silver ions in the hydroxyapatite crystal lattice caused a shift of specific HAP peaks to the left (towards smaller angles), confirming it substitutes calcium. The HAP peaks on the XRD pattern were broad, indicating the smaller particle size of the Ag/HAP powder compared to pure HAP powder.

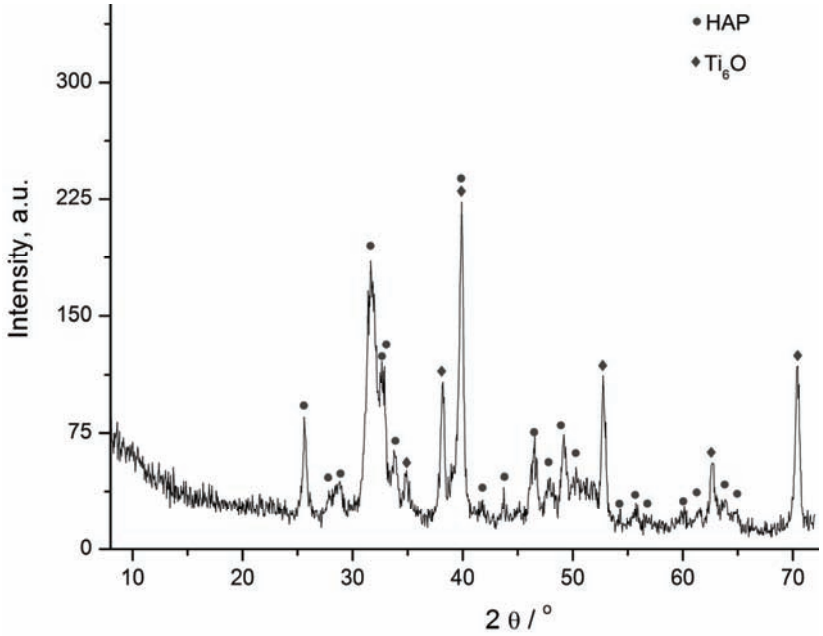

Fig. 1. XRD Pattern of an Ag/HAP coating electrodeposited on titanium.

Other specific peaks, matching titanium suboxide (JCPDS 72-1807), dominated the XRD spectrum instead of Ti peaks. This indicates that Ti was mainly present as Ti_6O on the coating surface. According to Chavan *et al.*,[14] the complex valence status of Ti is the result of oxygen diffusion from the exterior surface to the inside during air drying. Ti suboxides on the Ag/HAP surface are believed to be more active than TiO_2 in a physiological environment and can acti-

vate chemical bonding between the implant surface and adjacent biomolecules.[14] Therefore, the bioactivity of the material is more pronounced within the outermost surface, which not only has reactive functional groups of Ag/HAP, consisting of Ca^{+}, PO_4^{3-} and OH^{-}, but also of Ti suboxide to induce apatite nucleation in SBF.

SEM and EDS analysis

The surface morphology of the electrodeposited Ag/HAP coating on titanium and its EDS analysis are shown in Figs. 2a and 2b, respectively. The SEM microphotograph of the coating revealed the appearance of micro-cracks on the surface and also many agglomerates. The fractured surfaces were most probably formed due to shrinkage during the air drying. Although a cracked Ag/HAP layer would not protect the surface of an implant and thus allowing the possible release of titanium ions from the implant inside the body, the high magnification SEM micrograph (Fig. 2a) revealed that the width and depth of the cracks were in the nano range. Therefore, it is safe to assume that an Ag/HAP coating thus prepared would provide sufficient corrosion protection. On the other hand, the agglomerates on the coating surface would benefit the overall porosity.

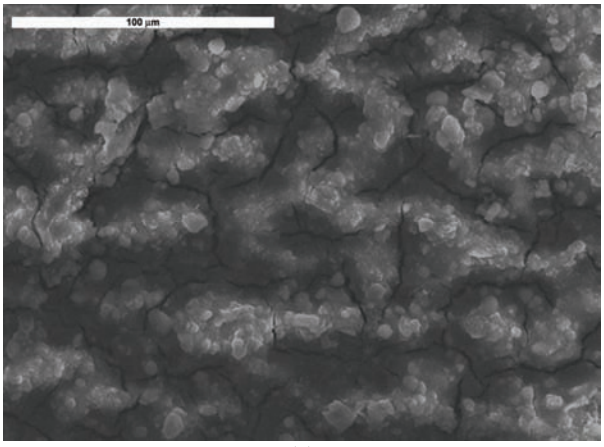

(a)

(b)

Fig. 2. a) SEM Microphotograph and b) EDS profile of the surface of an Ag/HAP coating electrodeposited on titanium.

Chavan *et al.*[14] reported that porous apatite layers could enhance the osteointegration and osteoconduction properties. In addition, it was reported that an open interconnected porous structure is advantageous as it enables penetration of the surrounding bone tissue and hence leads to better biointegration and mechanical stability at the interface of the surrounding bone and coated implants.[15]

The EDS spectra (Fig. 2b) showed two distinct peaks of Ca and P, also the presence of O peak and small peaks of Ti and Ag. The atomic ratio of Ca and P, obtained from the EDS profiling given in Table II was calculated to be 1.64, which is similar to the Ca/P ratio in human bone, known to be 1.67.[16]

TABLE II. The EDS composition of the Ag/HAP coating electrodeposited on titanium

Element	Intensity	Content, at. %
O K	0.662	69.35
P K	1.405	11.53
Ca K	1.024	18.92
Ti K	0.803	0.11
Ag L	0.766	0.08
Ca/P	–	1.64

ATR–FTIR Spectroscopy

The FTIR spectrum of the electrodeposited Ag/HAP coating on titanium and the assigned functional groups are illustrated in Fig. 3. As presented, all characteristic bands correspond to bands typical for hydroxyapatite.

The broad absorption bands at 3000–3500 cm^{-1} and the bending mode at 1613 cm^{-1} were assigned to O–H stretching and bending of H_2O in the spectrum of the Ag/HAP coating.[17] The OH^- stretching vibration was observed at 3572 cm^{-1}.[11] The most intensive band in the region from 1216–920 cm^{-1} was assigned to the P–O asymmetric stretching mode (ν_3) vibration of the PO_4^{3-} group[17–19] Other strong peaks observed as a doublet in the FTIR spectrum, located in 635––500 cm^{-1}, was derived from the triple (ν_4) degenerated bending modes of phosphate O–P–O bonds,[20] except for one of the weak characteristic band at 636 cm^{-1}, which corresponds to the vibration of the structural OH^- groups in the hydroxyapatite.[17]

A small sharp peak at 876 cm^{-1} was attributed to the presence of the HPO_4^{2-} group in the crystal lattice.[18,21] According to the literature, an improvement of the hydroxyapatite crystallinity could be observed by the transformation of the single band in the υ_4 region of the PO_4^{3-} group into a doublet band.[20]

It was reported that nano-sized hydroxyapatite particles, due to their size, have a very large surface area, enabling homogenous resorption by osteoclasts.[17] Therefore these coatings, due to the nano-sized Ag/HAP particles with improved crystallinity[22], as confirmed by the FTIR and XRD results, can present a suitable surface for the proliferation of bone cells.

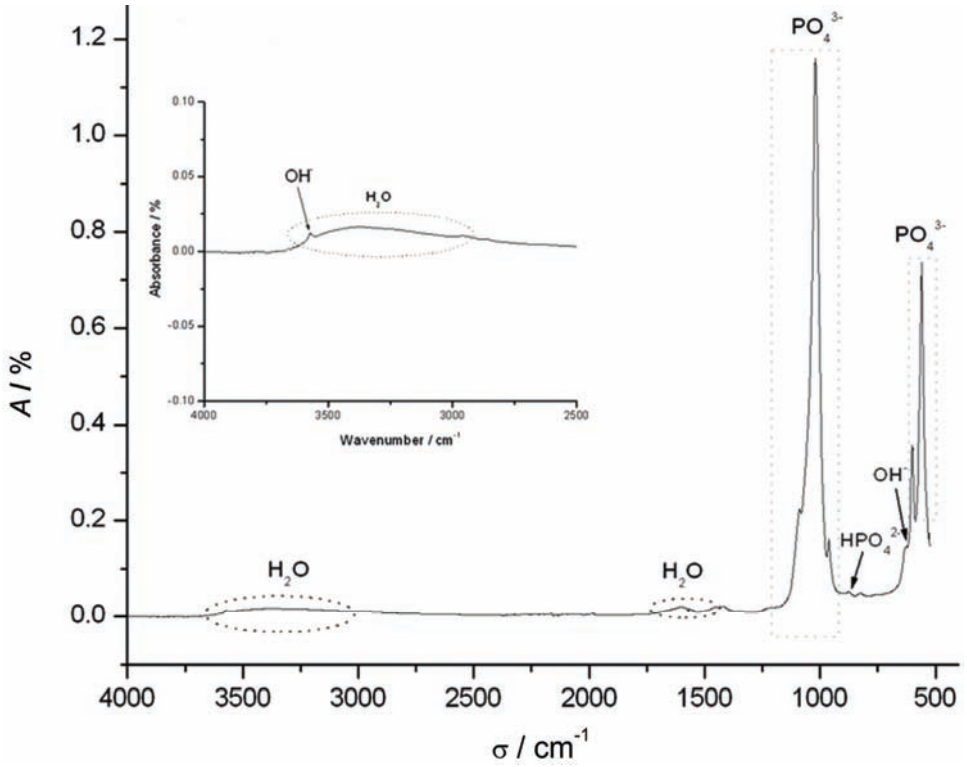

Fig. 3. ATR–FT-IR Spectrum of an Ag/HAP coating electrodeposited on titanium, in the wavenumber range 500–4000 cm^{-1} (inset: in the wavenumber range 2500–4000 cm^{-1}).

Thermogravimetric analysis

Depending on clinical need, nanosized crystalline hydroxyapatite can be used in various forms, including powders or particulate matter for drug delivery, filling bone voids, coatings for metallic prostheses, as scaffolds for bone grafts, drug delivery devices or in the development of composite biomaterials.[23] One of the important factors is the thermal stability of HAP in the temperature range of 400–1200 °C.[23] Therefore, it was necessary to study the thermal behaviour of the electrodeposited Ag/HAP coating scratched from Ti plates. The thermogravimetric (TG) and differential TG (DTG) curve (Fig. 4) revealed the weight loss of Ag/HAP with increasing temperature.

According to the TG and DTG curves, Figs. 4a and 4b, respectively, there are three distinct stages of weight loss. The first stage could be observed from 25 to 150 °C on the TG cure with a sharp peak on the DTG curve at 55 °C. This stage corresponds to desorption of adsorbed water from the surface of the Ag/ /HAP coating.[24]

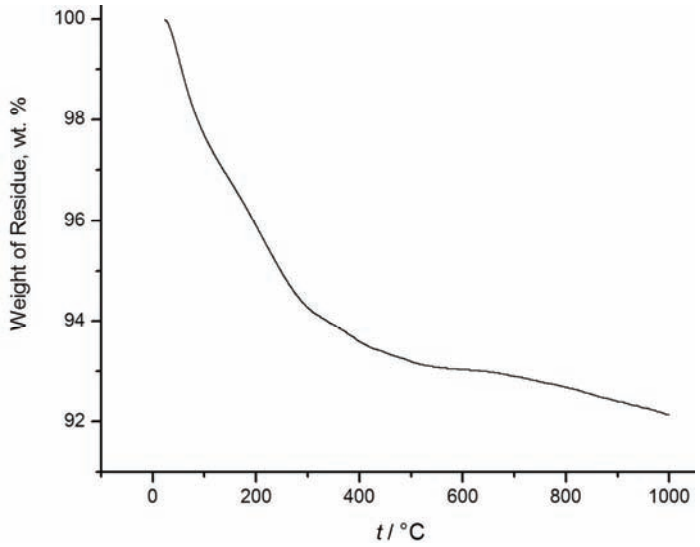

(a)

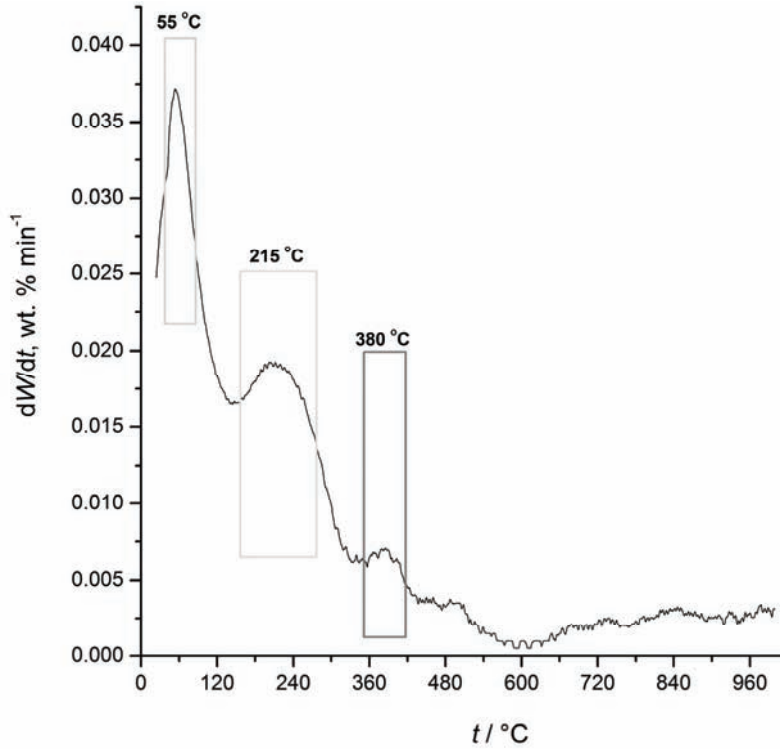

(b)

Fig. 4. a) TG and b) differential TG (DTG) curves of an Ag/HAP coating electrodeposited on titanium.

The second stage of weight loss on the TG curve was observed between 150 and 600 °C (Fig. 4a), with sharp peaks on the DTG curve at 215 and 380 °C (Fig. 4b), which can be attributed to the dehydroxylation of Ag/HAP.[25] As reported by Kalita and Verma,[23] all the endothermic peaks associated with this mass loss below 600 °C can be contributed to desorption of adsorbed water and possible elimination of crystal lattice water.

The third stage of the weight loss was observed between 600 and 1000 °C on the TG curve (Fig. 4a) but without distinguished peaks on the DTG plot. This phase could still be attributed to dehydroxylation or to the early slow decomposition of hydroxyapatite lattice.[26] The total weight loss for the Ag/HAP coating in the temperature range of 25–1000 °C was 7.9 wt. %.

EIS Studies of the corrosion behaviour in SBF solution

EIS measurements were used in order to study the corrosion behaviour of electrodeposited Ag/HAP coating on titanium in a physiological environment (SBF solution). The Nyquist plots of bare titanium and the electrodeposited Ag/HAP coating on titanium after 1 day and 3 days (Fig 5b). Compared to the Nyquist plot for the bare titanium after 1 day of immersion, on the Nyquist plot corresponding to the Ag/HAP coating on titanium after the same time of exposure (Fig. 5a), the semi-circle at the high frequency range (100 kHz–1 Hz) could be attributed to the Ag/HAP layer on the top, while the impedance response at the low frequencies range (1 Hz–10 mHz) showed the characteristics of a passive titanium oxide film beneath the Ag/HAP top layer.

The fitting of the experimental impedance data obtained from the Nyquist plots was accomplished using the equivalent electrical circuits shown in Figs. 6a and 6b and the Gamry Instruments Echem Analyst fitting program. The equivalent circuit in Fig. 6a was used for the fitting of impedance data obtained for the Ag/HAP coating (Fig. 5a). The assumed electrical equivalent circuit (Fig. 6a) consists of the electrolyte resistance, R_s, the coating pore resistance, *i.e.*, the resistance of the electrolyte inside the pores of Ag/HAP coating, R_p, the constant phase elements CPE_c and CPE_{pf}, which include all the frequency dependent electrochemical phenomena: the Ag/HAP coating capacitance, C_c, and the passive titanium oxide film capacitance, C_{pf}, respectively, and diffusion processes. The CPEs are used in this model to compensate non-homogeneity in the system and are defined by two parameters, Y_0 and n. The impedance of a CPE is represented by the following equation:[27–29]

$$Z_{CPE} = Y_0^{-1}(j\omega)^{-n} \quad (1)$$

where $j = (-1)^{1/2}$, $\omega = 2\pi f$ is the frequency in rad s^{-1} and f is the frequency in Hz. If the n value ranges from 0.8–1.0, the impedance of a CPE can be considered to be that of a pure capacitor:

$$Z_{\mathrm{CPE}} = (j\omega C)^{-n} \quad (2)$$

In the present case, the Y_0 value gave a pure capacitance (C). For impedance analysis of bare titanium, the equivalent circuit in Fig. 6b was used, where the electrolyte resistance is represented as R_s, the passive oxide film resistance and capacitance are R_{pf} and CPE_{pf}, respectively. All of the fitting results are listed in Table III.

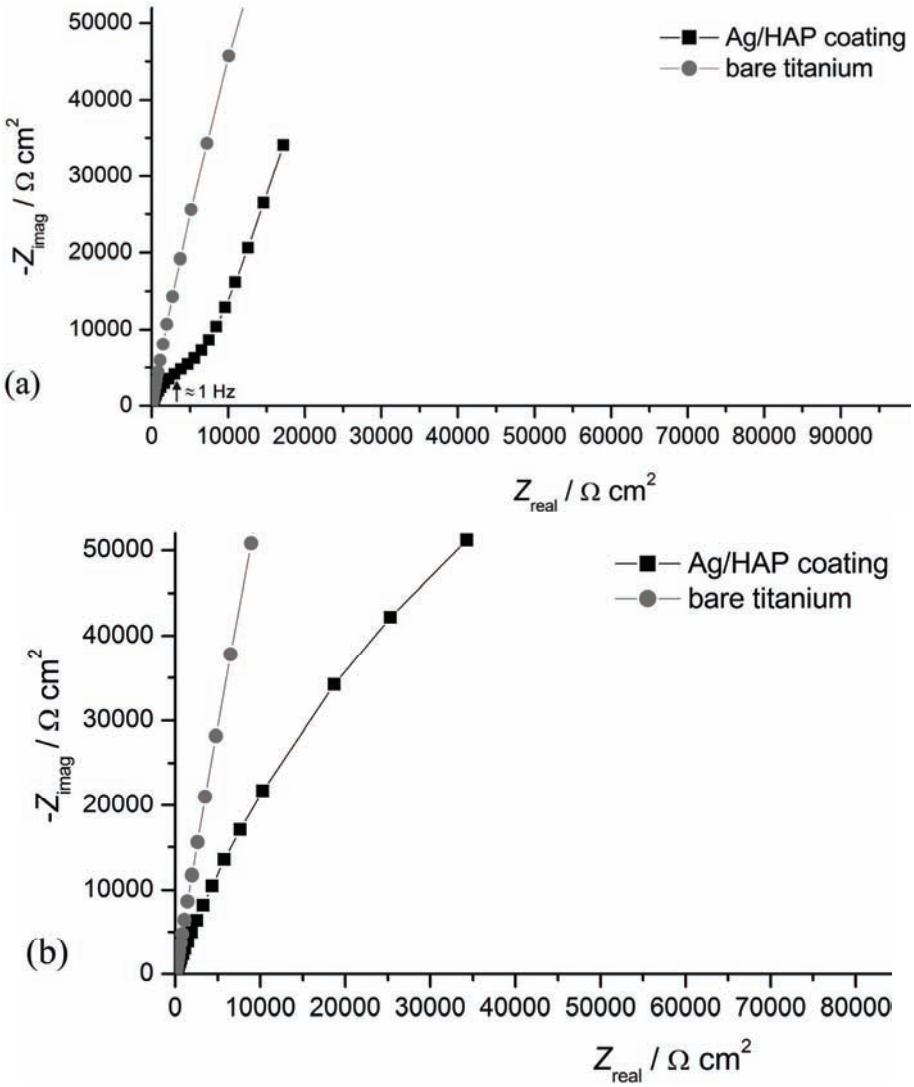

Fig. 5. The Nyquist plots of bare titanium and an Ag/HAP coating electrodeposited on titanium after a) 1 and b) 3 days of exposure to SBF solution at 37 °C.

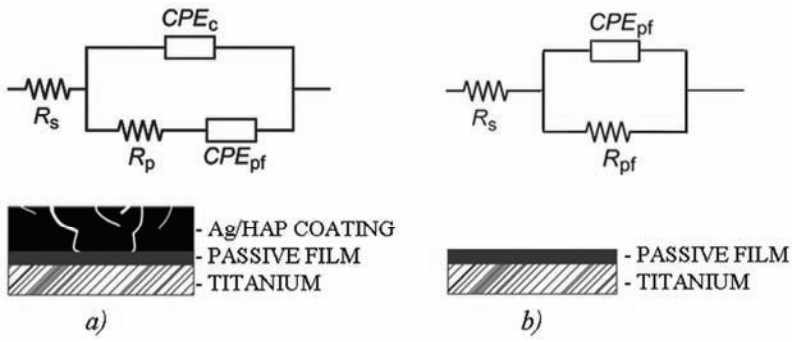

Fig. 6. Equivalent electrical circuits for a) an Ag/HAP coating electrodeposited on titanium and b) bare titanium.

TABLE III. The fitting values of the equivalent electrical circuits parameters

Sample	τ h	R_s Ω cm^2	CPE_{pf} (C_{pf}) μF cm^{-2}	n_{pf}	R_{pf} kΩ cm^2	CPE_C (C_C) μF cm^{-2}	n_C	R_p kΩ cm^2
Ag/HAP	1	31.6	220	0.77	–	89.5	0.83	12.6
	24	31.5	223	0.80	–	88.4	0.83	11.9
	72	51.4	147.2	0.78	240.7	–	–	–
Bare titanium	1	22.6	40.6	0.89	794	–	–	–
	24	22.5	38.8	0.89	1009	–	–	–
	72	67.8	26.6	0.90	3654	–	–	–

From Table III, as the n_c values in the case of Ag/HAP coating are higher than 0.8, CPE_c can be considered as the coating capacitance, C_c. The time dependence of the pore resistance, R_p, and the coating capacitance, C_c, of Ag/HAP coating are presented in Table III. According to the results, R_p and C_c for Ag/HAP coating remained constant during 24 h of exposure to the SBF solution, indicating retention of the good protective properties of the coating. However, after 72 h, the impedance Nyquist plot (Fig. 5b) could not be fitted with equivalent circuit shown in Fig. 6a and instead the equivalent circuit in Fig. 6b was used. The calculated values of R_{pf} (240.7 kΩ cm^2) and C_{pf} (147.2 μF cm^{-2}) after 72 h, given in Table III, could indicate the formation of a new apatite layer on the coating surface in SBF solution.[30] These results suggest that the coating pores filled with the SBF solution were growing into a very resistant passive film and on the other hand, the coating surface represented the site of nucleation and growth of new apatite.

The EIS spectra of the bare titanium exposed to SBF solution (Figs. 5a and 5b) was fitted to the equivalent electrical circuit shown in Fig. 6b. Its impedance plot exhibited behaviour similar to a capacitive response. Furthermore, a slow growth of the titanium oxide film could be traced through a slight decrease in the C_{pf} value and an increase in R_{pf} during 72 h of exposure to the SBF solution (Table III), which is in accordance with previously published data.[31]

In addition, this newly formed apatite that formed during immersion in SBF solution is known to accelerate better bonding between an implant and bone.[32]

CONCLUSIONS

A silver-doped hydroxyapatite Ag/HAP coating was successfully electrophoretically deposited on titanium. The XRD and ATR–FTIR results for the deposited coating showed there was no phase transformation of the hydroxyapatite lattice structure. The Ca/P ratio (from the EDS analysis) was calculated to be 1.64, as in natural bone. The analysis of the thermal behaviour of Ag/HAP coating revealed its stability up to 600 °C. Although SEM micrographs showed microcracks on the coating surface, the Ag/HAP coating provided sufficient corrosion protection during immersion in SBF solution, indicated by increase in pore resistance and decrease in coating capacitance.

Overall, not only did the Ag/HAP coating electrodeposited on titanium retain its protective properties in Kokubo's solution, but also expressed enhanced corrosion resistance due to formation of a bone-like apatite layer.

Acknowledgements. This research was financed by the Ministry of Education, Science and Technological Development of the Republic of Serbia, contract No. III 45019 and by the National Sciences and Engineering Research Council of Canada (NSERC). Dr Ana Jankovic was financed by the FP7 Nanotech FTM Grant Agreement 245916. The authors would like to thank Dr Miodrag Mitrić, Vinča Institute of Nuclear Sciences, University of Belgrade, for his help in the XRD measurements, and also to Mr Yves Bédard, Département des Sciences du bois et de la forêt de l'Université Laval, for technical support and assistance in the laboratory work.

И З В О Д

СПЕКТРОСКОПИЈА ЕЛЕКТРОХЕМИЈСКЕ ИМПЕДАНЦИЈЕ ПРЕВЛАКЕ ХИДРОКСИАПАТИТА ДОПИРАНЕ СРЕБРОМ У СИМУЛИРАНОЈ ТЕЛЕСНОЈ ТЕЧНОСТИ КОРИШЋЕНОЈ КАО КОРОЗИОНИ АГЕНС

АНА ЈАНКОВИЋ[1], САЊА ЕРАКОВИЋ[1], ANTONIJA DINDUNE[2], ЂОРЂЕ ВЕЉОВИЋ[1], ТАТЈАНА СТЕВАНОВИЋ[3], ЂОРЂЕ ЈАНАЋКОВИЋ[1] и ВЕСНА МИШКОВИЋ-СТАНКОВИЋ[1]

[1]Технолошко–металуршки факултет, Универзитет у Београду, Карнегијева 4, Београд, [2]Institute of Inorganic Chemistry, Riga Technical University, 34 Miera Street, Salaspils, LV-2169, Latvia и [3]Département des sciences du bois et de la forêt, Université Laval, 2425 rue de la Terrasse, Québec, Canada

Титан представља кључни биомедицински материјал захваљујући својој доброј биокомпатибилности, механичким својствима и корозионој стабилности, али инфекције на месту имплантирања и даље представљају озбиљан проблем. Један начин да се предупреди инфекција је да се побољша антимикробна активност материјала. Сребром допиране наночестице хидроксиапатита синтетисане су новом модификованом преципитационом методом. Овако синтетисани прах је коришћен за наношење превлаке сребро/хидроксиапатит на титан електофоретским таложењем. Фазни састав и структура превлаке су карактерисани спектроскопијом инфрацрвене светлости са Фуријеовом трансформацијом у моду тоталне рефлексије и дифракцијом X-зрака. Морфологија површине и хемијски састав испитивани су коришћењем скенирајуће електронске микро-

скопије и енергетске дисперзионе спектроскопије. Циљ истраживања је испитивање корозионе стабилности превлаке сребро/хидроксиапатит у симулираној телесној течности користећи спектроскопију електрохемијске импеданције. Превлака сребро/хидроксиапатит обезбеђује добру заштиту од корозије у симулираној телесној течности.

(Примљено 12. јула, ревидирано 27. августа 2012)

REFERENCES

1. C. Moseke, U. Gbureck, P. Elter, P. Drechsler, A. Zoll, R. Thull, A. Ewald, *J. Mater. Sci. - Mater. Med.* **22** (2011) 2711
2. Y.-T. Sul, C. B. Johansson, S. Petronis, A. Krozer, Y. Jeong, A. Wennerberg, T. Albrektsson, *Biomaterials* **23** (2002) 491
3. K. G. Neoh, X. Hu, D. Zheng, E. T. Kang, *Biomaterials* **33** (2012) 2813
4. L. Zhao, P. K. Chu, Y. Zhang, Z. Wu, *J. Biomed. Mater. Res., B* **91** (2009) 470
5. C. Garcia, S. Cere, A. Duran, *J. Non-Cryst. Solids* **352** (2006) 3488
6. K.-C. Kung, T.-M. Lee, T.-S. Lui, *J. Alloys Compd.* **508** (2010) 384
7. P. C. Rath, L. Besra, B. P. Singh, S. Bhattacharjee, *Ceram. Int.* **38** (2012) 3209
8. M. Geetha, A. K. Singh, R. Asokamani, A. K. Gogi, *Prog. Mater. Sci.* **54** (2009) 397
9. M. Swetha, K. Sahithi, A. Moorthi, N. Srinivasan, K. Ramasamy, N. Selvamurugan, *Int. J. Biol. Macromol.* **47** (2010) 1
10. M. S. Djosić, V. B. Mišković-Stanković, V. V. Srdić, *J. Serb. Chem. Soc.* **72** (2007) 275
11. M. S. Lazić, K. Simović, V. B. Mišković-Stanković, P. Jovanić, D. Kićević, *J. Serb. Chem. Soc.* **69** (2004) 239
12. V. B. Mišković-Stanković, *J. Serb. Chem. Soc.* **67** (2002) 305
13. A. A. Abdeltawab, M. A. Shoeib, S. G. Mohamed, *Surf. Coat. Tech.* **206** (2011) 43
14. P. N. Chavan, M. M. Bahir, R. U. Mene, M. P. Mahabole, R. S. Khairnar, *Mater. Sci. Eng., B* **168** (2010) 224
15. M. Javidi, S. Javadpour, M. E. Bahrololoom, J. Ma, *Mater. Sci. Eng., C* **28** (2008) 1509
16. B. Cengiz, Y. Gokce, N. Yildiz, Z. Aktas, A. Calimli, *Colloid. Surf., A* **322** (2008) 29
17. K. P. Sanosh , M.-C. Chu , A. Balakrishnan , Y.-J. Lee, T. N. Kim , S.-J. Cho, *Curr. Appl. Phys.* **9** (2009) 1459
18. L.-N. Wang, J.-L. Luo, *Mater. Sci. Eng., C* **31** (2011) 748
19. D. K. Pattanayak, R. Dash, R. C. Prasad, B. T. Rao, T. R. Rama Mohan, *Mater. Sci. Eng., C* **27** (2007) 684
20. H. Ye, X. Y. Liu, H. Hong, *Mater. Sci. Eng.,C* **29** (2009) 2036
21. E. V. Pecheva, L. D. Pramatarova, M. F. Maitz, M. T. Pham, A. V. Kondyuirin, *Appl. Surf. Sci.* **235** (2004) 176
22. S. Eraković, Đ. Veljović, P. N. Diouf, T. Stevanović, M. Mitrić, S. Milonjić, V. Mišković-Stanković, *Int. J. Chem. React. Eng.* **7** (2009) *Article* A62
23. S. J. Kalita, S. Verma, *Mater. Sci. Eng., C* **30** (2010) 295
24. T. Wang, A. Dorner-Reisel, E. Muller, *J. Eur. Ceram. Soc.* **24** (2004) 693
25. X. Zhang, Y. Li, G. Lv, Y. Zuo, Y. Mu, *Polym. Degrad. Stabil.* **91** (2006) 1202
26. S. Eraković, Dj. Veljović, P. N Diouf, T. Stevanović, M. Mitrić, Dj. Janaćković, I. Z. Matić, Z. D Juranić, V. B. Mišković-Stanković, *Prog. Org. Coat.* **75** (2012) 275
27. M. M. Popović, B. N. Grgur, V. B. Mišković-Stanković, *Prog. Org. Coat.* **52** (2005) 359
28. M. Sluyters-Rehbach, *Pure Appl. Chem.* **66** (1994) 1831
29. V. D. Jović, B. M. Jović, *J. Electroanal. Chem.* **541** (2003) 1

30. S. Eraković, A. Janković, Dj. Veljović, E. Palcevskis, M. Mitrić, T. Stevanović, Dj. Janaćković, V. Mišković-Stanković, *J. Phys. Chem. B*, http://pubs.acs.org/doi/abs/ /10.1021/jp305252a.
31. L. Jonasova, F. A. Muller, A. Helebrant, J. Strnad, P. Greil, *Biomaterials* **25** (2004) 1187
32. G. Manivasagam, D. Dhinasekaran, A. Rajamanickam, *Recent Pat. Corr. Sci.* **2** (2010) 40.